ChemComm

COMMUNICATION

View Article Online
View Journal | View Issue

Cite this: *Chem. Commun.*, 2022, **58**, 9766

Received 10th June 2022,
Accepted 23rd June 2022

DOI: 10.1039/d2cc03256b

rsc.li/chemcomm

Facile high-yield synthesis and purification of lysine-modified graphene oxide for enhanced drinking water purification†

Sebastiano Mantovani,‡[a] Sara Khaliha,‡[a] Tainah Dorina Marforio,‡[b] Alessandro Kovtun,[a] Laura Favaretto,[a] Francesca Tunioli,[a] Antonio Bianchi,[a] Gaetana Petrone,[c] Andrea Liscio,[c] Vincenzo Palermo,*[a] Matteo Calvaresi,*[b] Maria Luisa Navacchia[a] and Manuela Melucci*[a]

Lysine–covalently modified graphene oxide (GO-Lys) was prepared by an innovative procedure. Lysine brushes promote enhanced adsorption of bisphenol A, benzophenone-4 and carbamazepine contaminants from tap water, with a removal capacity beyond the state of the art.

Graphene oxide nanosheets (GO) have been widely investigated in the last few years as sorbents for several organic molecules and heavy metal ions in water.[1–3] The abundant surface chemical groups, combined with the large surface area available for adsorption, have resulted in faster adsorption kinetics and efficiency toward several classes of pollutants, including emerging concern contaminants, in comparison to other carbon-based nanomaterials such as active carbon, the standard industrial sorbent.[4] These contaminants are a matter of great concern because of their persistence, mobility in water bodies and health and environmental toxicity.[5–7] The carboxylic and carbonyl groups of GO nanosheets play an important role in the adsorption efficiency of organic molecules, since they enable H-bonds and metal ion complexation.[2,3] In addition, chemical modification of such surface groups can be exploited for promoting selective adsorption capability. For instance, polyethyleneimine (PEI) modification has been reported as a successful strategy to adsorb metal cations,[8] organic molecules and arsenic anions[2] from tap water thanks to the synergy of π-stacking, complexation and electrostatic interactions enabled by GO and PEI structures. On this line, here we report the synthesis of a lysine-modified GO (GO-Lys) and the study of its potential for water remediation. Amino acid-modified GO has been proposed in recent years as a material with enhanced biocompatibility[9] (methionine), anti-corrosion (lysine), lead adsorption,[10] and antibiotic (methionine, cysteine) or dye adsorption[11,12] properties. Nanocomposites of amino acid-GO have been also exploited for magnetic separation of proteins[13] (L-arginine, glutamic acid, phenylalanine, and cysteine), for the fabrication of membranes for direct methanol fuel cells[14] (aspartic acid) or as coatings of electrodes for biosensing applications (methionine).[15] The synthesis of such modified GO has been generally carried out by amidation after GO carboxylic acid activation by 1-ethyl-3-(3-dimethylaminopropyl)carbodiimide (EDC) or thionyl chloride ($SOCl_2$), followed by reaction with the amino groups. Alternatively, epoxide ring opening reaction by the nucleophilic amino group of the amino acid has also been proposed.[16,17] On this line, aiming at advanced design strategies able to promote specific sorption properties, we report a study on GO-Lys nanosheets for drinking water purification. GO-Lys was synthesized by microwave (MW)-activated amination§ and purified using a new convenient microfiltration (MF) protocol. The adsorption selectivity and efficiency of GO-Lys toward a selection of contaminants of emerging environmental concern, as a mixture in tap water (including drugs and dyes, whose molecular structures are reported in Fig. S1, ESI†), were investigated by combined kinetic/isotherm adsorption studies and molecular modelling. In particular, the adsorption mechanism and capacity toward three emerging water contaminants, *i.e.* bisphenol A (BPA), a plastic additive; carbamazepine (CBZ), an anti-epileptic drug; and benzophenone-4 (BP4), a sunscreen ingredient, were deeply investigated (Tables S1–S3, ESI†).

The synthetic route to GO-Lys is shown in Scheme 1. In the experimental conditions (pH 9.0), the reaction is expected to involve exclusively the alpha NH_2 group, having a pK_a of 8.95 (the side chain amine has a pK_a of 10.79).[18,19] We also carried

[a] *Consiglio Nazionale delle Ricerche, Institute of Organic Synthesis and Photoreactivity (CNR-ISOF) via Piero Gobetti 101, 40129 Bologna, Italy. E-mail: manuela.melucci@isof.cnr.it*
[b] *Alma Mater Studiorum - University of Bologna, Department of Chemistry 'G. Ciamician', via Selmi 2, 40129 Bologna, Italy*
[c] *Consiglio Nazionale delle Ricerche, Institute for Microelectronics and Microsystems (CNR-IMM), via del fosso del cavaliere 100, 00133 Roma, Italy*

† Electronic supplementary information (ESI) available: Contaminants' structures and the state of the art removal, synthesis, XPS, ATR-FTIR, morphology, TGA, HPLC, computational details, and adsorption isotherms. See DOI: https://doi.org/10.1039/d2cc03256b

‡ These authors contributed equally to this work.

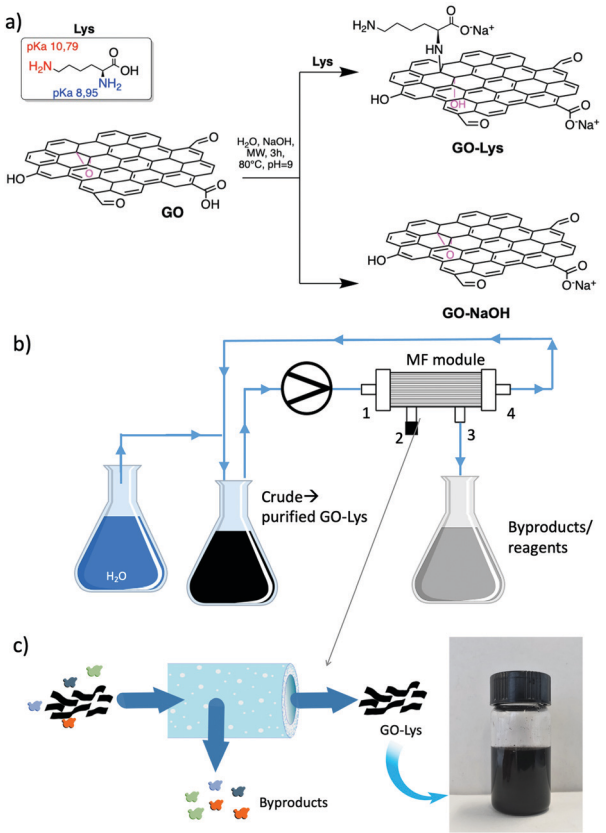

Scheme 1 (a) Synthetic route to GO-Lys and GO-NaOH, (b) sketch of the purification of GO-Lys by microfiltration, and (c) zoomed-in view of the microfiltration procedure and image of the GO-Lys suspension (2 mg mL^{-1} after 30 h from sonication).

out the reaction on GO without the addition of lysine to prepare GO-NaOH as a reference compound and to exclude any possible effect on the adsorption derived from exfoliation or structural changes promoted by the reaction conditions. For purification, we exploited microfiltration on commercial Versatile™ PES modules (Plasmart 100, Medica Spa).

Such modules have a filtering surface of about 0.1 m^2, and cut-off of 150 nm. The dead end in-out procedure (*i.e.* inlet by point 1 and out by point 3, 2/4 exits were closed), previously reported,[2] was here improved by working in the loop-dead end modality, as shown in Scheme 1b and c. The crude suspension was flowed through the inner fiber lumen (inlet by point 1, out by points 3 and 4, and recirculation by point 4) and recirculated, while small molecules of size below the fiber pores pass by the fiber section (exit 3). Clean water was progressively added to the crude to purify the modified GO until a neutral pH was measured for the collected GO-Lys solution. The total added volume of water was about 1.5 L/300 mg GO starting material for our procedure with respect to 2.3 L/300 mg required for conventional reiterated centrifugation-based purification. This microfiltration protocol allowed us to speed up the filtration by working at a higher flow rate (100 mL min^{-1}), with respect to the previously reported dead-end in-out microfiltration procedure, which works at a maximum of 20 mL min^{-1}.[2]

In addition, by working in the loop modality, we did not observe clogging of the pores of the membranes, as instead observed in the dead-end closed modality.[2] The overall procedure resulted in (i) less water/time consumption than centrifugation, (ii) less energy demand, and (iii) less mechanical detriment for the modules than those of the previously reported microfiltration procedure.[2] Moreover, the cartridges being commercially available with larger size and higher filtering surface, the process could be easily upscaled. GO-Lys composition, surface charge and morphology were characterized, and its properties compared to those of pristine GO and GO-NaOH reference materials. Almost preserved solubility and stability in water were observed for GO-Lys when compared to GO (Scheme 1c). The ζ potential values of GO-Lys (-35.2 ± 0.8 mV) were slightly more positive than that of GO (-43.1 ± 2.4 mV), as expected. X-ray photoelectron spectroscopy (XPS) of GO-Lys revealed the increase of nitrogen (N 1s at 400 eV), compared to that of pristine GO, with a nitrogen content of 3.2%, in accordance with elemental analysis results (N content 36%). A lysine loading of 16% was estimated by considering the atomic composition of L-lysine. The survey spectra of GO, GO-NaOH and GO-Lys are reported in Fig. 1 and their atomic composition is reported in Table S4, ESI.† The ATR-FTIR spectrum of GO-Lys (Fig. S2, ESI†) shows the typical peak of GO (O–H stretching vibrations) at 3700–2500 cm^{-1}, which is likely to be overlapping to the N–H stretching. The disappearance of the CO stretching at 1720 cm^{-1} and the increase of the band at 1570 cm^{-1} (C=C stretching modes) were found in both the GO-NaOH and GO-Lys spectra, likely due to the reduction occurring under the experimental conditions.[17] The absence of amidic C=O stretching at *ca.* 1650 cm^{-1} also excludes the occurrence of side amidation reactions on the carboxylic groups and supports the epoxide ring opening reaction, in good accordance with the NMR studies previously reported by Bianco *et al.*[17] TGA analysis revealed the presence of an inflection point at 372 °C (peak in derivative) ascribed to lysine and absent in the control sample GO-NaOH (Fig. S3 and S4, ESI†). Scanning electron microscopy (SEM, Fig. S5, ESI†) of GO-Lys revealed agglomerates of multiple micron-sized flexible flakes consisting of overlapped and randomly oriented sheets. The GO-Lys nanosheet morphology was comparable to

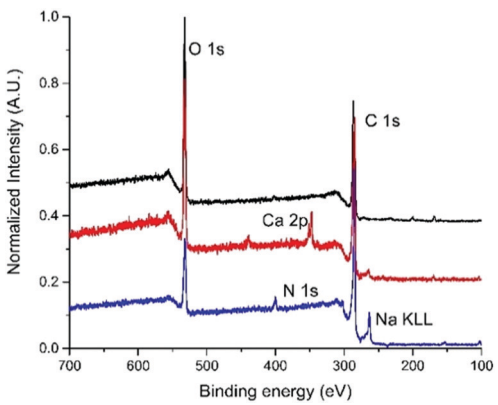

Fig. 1 Survey spectra of GO (black line), GO-NaOH (red line) and GO-Lys (blue line).

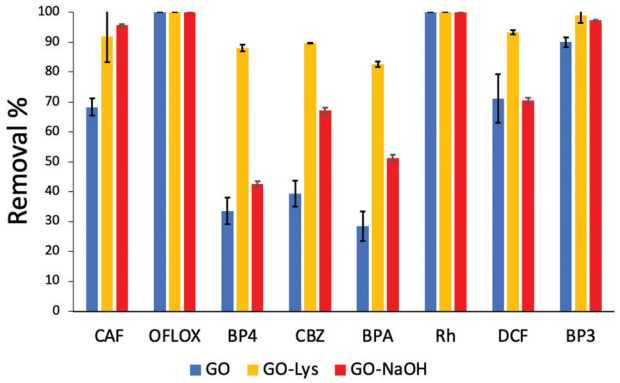

Fig. 2 Removal of EC mix (5 ppm each, V_{tot} = 25 mL^{-1}, 25 mg of sorbent, contact time 24 h (data at 1 h and 4 h are reported in Fig. S7 and S8 ESI†). The acronyms refer to the molecules shown in Fig. S1, ESI.†

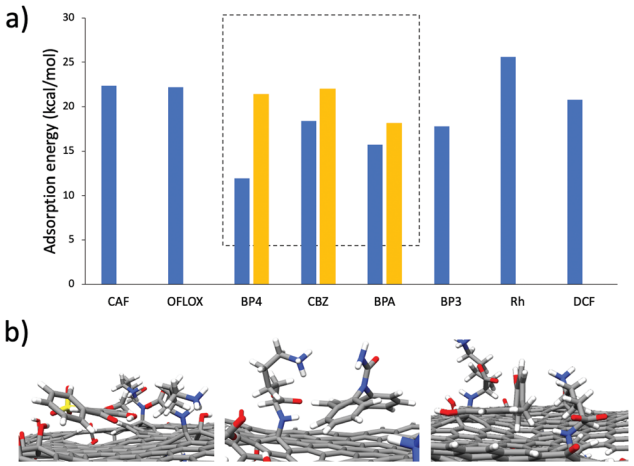

Fig. 3 (a) Binding affinity of ECs with GO (blue bars) and GO-Lys (yellow bars) calculated by the MM-GBSA approach. (b) Representative snapshots from MD simulations (the most interacting snapshot was selected) of BP4, CBZ and BPA on the GO-Lys sheet. The acronyms refer to the molecules shown in Fig. S1, ESI.†

that of GO, with lateral size spanning between 10 nm and 300 nm, and a mean value of 60 nm, in good agreement with the values measured for GO nanosheets produced *via* the modified Hummers method[20] (Fig. S6 and Table S5, ESI†). Adsorption kinetic experiments on the mixture of ECs (structure in Fig. S1, ESI†) were carried out by dispersing GO, GO-Lys and GO-NaOH nanosheets (after sonication for 2 h) in spiked tap water and analysing treated water samples after 1 h, 4 h, and 24 h by HPLC analysis (details in ESI†). Fig. 2a shows the removal after 24 h, while the histograms at 1 h and 4 h are reported in Fig. S7 and S8, ESI.† A marked different selectivity can be seen for GO-Lys in the adsorption of BP4, BPA and CBZ, with higher removal (>80%) than for GO (<40%) and GO-NaOH (40–65%).

Due to the high adsorption differences observed, these three molecules were selected as a case study to understand the different selectivity of GO-Lys. To this aim, molecular dynamics (MD) simulations were used to explain the observed molecular selectivity and get some insight on molecule-graphene interaction. MD simulations might identify the favourite adsorption sites on graphene and, through Molecular Mechanics-Generalized Born Surface Area (MM-GBSA) analysis, quantify their binding energies.[21,22] The calculated interaction energies of the eight compounds with GO (Fig. 3a) show that BP4, CBZ and BPA are characterized by the smallest values, reflecting the lower adsorption values experimentally observed (Fig. 2) for these molecules. When the calculation is repeated with GO-Lys, an increase of the binding affinity is observed, in agreement with the experimental results. Interestingly, the MM-GBSA analysis (Tables S5 and S6, ESI†) results revealed that the driving forces governing the interaction between the molecules and the graphene sheets were enhanced van der Waals interactions between the BP4, CBZ and BPA compounds and GO-Lys (Fig. S9 and Table S7, ESI†). Indeed, the lysine residues, laying down on the graphene sheet, create a local "corrugation" on the basal plane of graphene,[23] able to improve the interaction with non-planar/bent molecules, such as BP4, CBZ and BPA. The 3D recognition sites (Fig. 3b) created by lysine grafting increase the shape complementarity between the nano sorbent and the contaminant molecules, contributing to the observed adsorption capacity enhancement.[3,24,25] In parallel to MD simulations, to understand the different selectivity of GO-Lys for BP4, CBZ and BPA, adsorption isotherms were performed for each material (Fig. 4, details in Tables S8–S10, ESI†). Isotherm curves are shown in Fig. 4. Two models were used for fitting the isotherms: (i) the BET model considers a multilayer adsorption, where the molecule–molecule interaction is similar to the molecule substrate one, while (ii) the Langmuir model considers only a single monolayer and a much stronger molecule-substrate interaction. All molecules were adsorbed by GO-Lys in accordance with the Langmuir model, while both the Langmuir and BET models described the adsorption mechanism on GO. The Langmuir adsorption model suggests that the

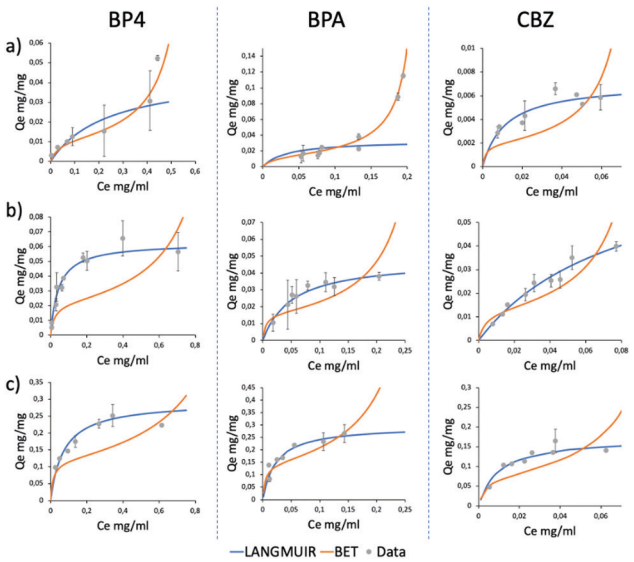

Fig. 4 Adsorption isotherms of GO (a), GO-NaOH (b) and GO-Lys (c) for BP4, BPA and CBZ (from left to right). Blue lines, Langmuir model; red lines, BET model.

Table 1 Summary of the maximum adsorption capacities of GO, GO-NaOH and GO-Lys estimated by the isotherm curves (best fitting model). Regular text, Langmuir model; italic text, BET model

	GO	GO-NaOH	GO-Lys
Q_m BP4 (mg g^{-1})	*11 ± 5*	62 ± 12	292 ± 30
Q_m BPA (mg g^{-1})	*14 ± 5*	48 ± 15	295 ± 50
Q_m CBZ (mg g^{-1})	7 ± 2	80 ± 15	172 ± 20

interactions between BP4, CBZ, and BPA molecules and GO-Lys are stronger than the molecule–molecule interaction (details in Tables S11–S13, ESI†), in good accordance with previously reported sorption studies of the same molecules on carbon sorbents, such as activated carbon, multiwalled carbon nanotubes, and expanded graphite (details in Table S1–S3, ESI†). The observed maximum adsorption capacity trends (Q_m, Table 1) were in good accordance with kinetic experiment results (the correlation plot between experimental Q_m and calculated binding affinity is reported in Fig. S10, ESI†). The Q_m values of GO-Lys for BP4, BPA and CBZ overcome the ones obtained for GO and GO-NaOH, showing adsorption capacities under 100 mg g^{-1}. Noteworthily, the estimated Q_m values are from 2 to 20 (BP4, CBZ, and BPA) times higher than the state of the art values reported for other materials, such as reduced GO nanosheets[26] (Q_m BPA = 181 mg g^{-1}), polypyrrole-chitosan-Fe_3O_4 nanoparticles[27] (Q_m CBZ = 122 mg g^{-1}), and amine functionalized resins[28] (Q_m BP4 = 154 mg g^{-1}) (Tables S1–S3, ESI†). In conclusion, GO-Lys was prepared by microvawe promoted amination and purified with an innovative microfiltration-based protocol, allowing fast, high yield purification of modified graphene nanosheets. The procedure allowed a loading of lysine of about 16%, preserving the morphology and the solubility of GO. Lysine modification allowed enhanced removal of BPA, CBZ and BP4, three water contaminants of growing environmental concern. Molecular modelling ascribed the observed removal enhancement to higher van der Waals interactions between GO-Lys and BP4, CBZ and BPA molecules. Adsorption isotherms revealed maximum capacity of up to twenty times higher than those of the already reported nano sorbents (Tables S1–S3, ESI†). The high performance combined with (i) simple preparation and purification protocols, and (ii) lysine biocompatibility and eco sustainability opens the way to the development of GO-Lys composites, such as membranes and foams, for drinking water purification scenarios. Studies in this direction are currently under way.

The authors gratefully acknowledge support of this work through the projects 825207-GO-FOR-WATER and 881603-GrapheneCore3-SH-GRAPHIL. MM thanks Dr L. Bocchi and M. Fecondini (Medica SpA) for providing Versatile™ PES modules.

Conflicts of interest

There are no conflicts to declare.

Notes and references

§ *Synthesis and purification of GO-Lys*. A basic solution of L-lysine was prepared by adding 930 mg of Lys (6.36 mmol) and 381 mg of NaOH (9.53 mmol) in MilliQ water (13 mL). The solution was then added to 62 mL of GO suspension (5 mg mL^{-1} in MilliQ water, sonicated for 2 h) and the mixture was irradiated with MW for 1 h (T_{max} = 80 °C; P_{max} = 120W. EtOH (5 mL) was added and the crude was purified by MF (Plasmart 100, Medica SpA) in loop filtration modality (in-out, Scheme 1b) by using a peristaltic pump at 100 mL min^{-1}. Pure water was progressively added to the feed solution (total volume = 1,5 L). The process was stopped when a neutral pH was measured in the permeated water. 263 mg of GO-Lys was obtained after drying.

1 F. Perreault, A. Fonseca de Faria and M. Elimelech, *Chem. Soc. Rev.*, 2015, **44**, 5861–5896.
2 S. Mantovani, S. Khaliha, L. Favaretto, C. Bettini, A. Bianchi, A. Kovtun, M. Zambianchi, M. Gazzano, B. Casentini, V. Palermo and M. Melucci, *Chem. Commun.*, 2021, **57**, 3765–3768.
3 S. Khaliha, T. D. Marforio, A. Kovtun, S. Mantovani, A. Bianchi, M. Luisa Navacchia, M. Zambianchi, L. Bocchi, N. Boulanger, A. Iakunkov, M. Calvaresi, A. V. Talyzin, V. Palermo and M. Melucci, *FlatChem*, 2021, **29**, 100283.
4 C. Backes, *et al.*, *2D Mater.*, 2020, **7**, 022001.
5 J. M. Diamond, H. A. Latimer II, K. R. Munkittrick, K. W. Thornton, S. M. Bartell and K. A. Kidd, *Environ. Toxicol. Chem.*, 2011, **30**, 2385–2394.
6 G. Bertanza, G. U. Capoferri, M. Carmagnani, F. Icarelli, S. Sorlini and R. Pedrazzani, *Sci. Total Environ.*, 2020, **734**, 139154.
7 Z. Liew and P. Guo, *Science*, 2022, **375**, 720–721.
8 D. Pakulski, W. Czepa, S. Witomska, A. Aliprandi, P. Pawluć, V. Patroniak, A. Ciesielski and P. Samorì, *J. Mater. Chem. A*, 2018, **6**, 9384–9390.
9 A. O. E. Abdelhalim, V. V. Sharoyko, A. A. Meshcheriakov, M. D. Luttsev, A. A. Potanin, N. R. Iamalova, E. E. Zakharov, S. V. Ageev, A. V. Petrov, L. V. Vasina, I. L. Solovtsova, A. V. Nashchekin, I. V. Murin and K. N. Semenov, *J. Mol. Liq.*, 2020, **314**, 113605.
10 H. Ge and W. Zou, *J. Dispersion Sci. Technol.*, 2017, **38**, 241–247.
11 S. Yadav, A. Asthana, A. K. Singh, R. Chakraborty, S. S. Vidya, A. Singh and S. A. C. Carabineiro, *Nanomaterials*, 2021, **11**, 568.
12 J. Xiao, W. Lv, Z. Xie, Y. Song and Q. Zheng, *J. Mater. Sci.*, 2017, **52**, 5807–5821.
13 M. Yan, Q. Liang, W. Wan, Q. Han, S. Tan and M. Ding, *RSC Adv.*, 2017, **7**, 30109–30117.
14 G. Rambabu and S. D. Bhat, *J. Membr. Sci.*, 2018, **551**, 1–11.
15 W. Qiao, L. Wang, B. Ye, G. Li and J. Li, *Analyst*, 2015, **140**, 7974–7983.
16 K. Spyrou, M. Calvaresi, E. K. Diamanti, T. Tsoufis, D. Gournis, P. Rudolf and F. Zerbetto, *Adv. Funct. Mater.*, 2015, **25**, 263–269.
17 I. A. Vacchi, C. Spinato, J. Raya, A. Bianco and C. Ménard-Moyon, *Nanoscale*, 2016, **8**, 13714–13721.
18 C. B. Rosen and M. B. Francis, *Nat. Chem. Biol.*, 2017, **13**, 697–705.
19 L. De Rosa, R. Di Stasi, A. Romanelli and L. D. D'Andrea, *Molecules*, 2021, **26**, 3521.
20 A. Liscio, K. Kouroupis-Agalou, X. D. Betriu, A. Kovtun, E. Treossi, N. M. Pugno, G. De Luca, L. Giorgini and V. Palermo, *2D Mater.*, 2017, **4**, 025017.
21 M. Calvaresi, A. Bottoni and F. Zerbetto, *J. Phys. Chem. C*, 2015, **119**, 28077–28082.
22 M. Di Giosia, T. D. Marforio, A. Cantelli, F. Valle, F. Zerbetto, Q. Su, H. Wang and M. Calvaresi, *J. Colloid Interface Sci.*, 2020, **571**, 174–184.
23 J. Wang, B. Chen and B. Xing, *Environ. Sci. Technol.*, 2016, **50**, 3798–3808.
24 M. Calvaresi, S. Furini, C. Domene, A. Bottoni and F. Zerbetto, *ACS Nano*, 2015, **9**, 4827–4834.
25 M. Di Giosia, F. Valle, A. Cantelli, A. Bottoni, F. Zerbetto, E. Fasoli and M. Calvaresi, *Carbon*, 2019, **147**, 70–82.
26 J. Xu, L. Wang and Y. Zhu, *Langmuir*, 2012, **28**, 8418–8425.
27 A. Nezhadali, S. E. Koushali and F. Divsar, *J. Environ. Chem. Eng.*, 2021, **9**, 105648.
28 X. Zhou, Y. Yang, C. Li, Z. Yang, W. Yang, Z. Tian, L. Zhang and T. Tao, *J. Cleaner Prod.*, 2018, **203**, 655–663.